Full Paper

Journal of the Brazilian Chemical Society

https://dx.doi.org/10.21577/0103-5053.20260056

J. Braz. Chem. Soc. **2026**, *37-Spe1*, e-20260056, 1-11

^{1}H HR-MAS NMR Metabolomics Uncovers Coordinated Metabolic Response to Water Stress in Transgenic Swingle Citrumelo

Caroline S. Oliveira, [a] ***Paola D. Oliveira,*** [a] ***Rafael P. Apparecido,*** [a] ***Luiz G. E. Vieira,*** [b] ***Luciano M. Lião,*** [c] ***Eduardo F. Carlos*** [d] ***and Glaucia B. Alcantara*** *,[a]

[a]*Laboratório de Pesquisa LP2, Instituto de Química, Universidade Federal de Mato Grosso do Sul, 79074-460 Campo Grande-MS, Brazil*

[b]*Universidade do Oeste Paulista, 19067-175 Presidente Prudente-SP, Brazil*

[c]*Laboratório de RMN, Instituto de Química, Universidade Federal de Goiás, 74690-900 Goiânia-GO, Brazil*

[d]*Solo Sagrado Agronegócios, 13855-050 Mogi Guaçu-SP, Brazil*

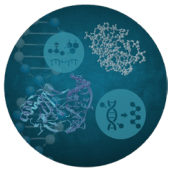

Understanding the biochemical mechanisms underlying drought tolerance in citrus is essential for developing rootstocks adapted to water-deficit conditions. This study applied proton high resolution magic-angle spinning nuclear magnetic resonance (^{1}H HR-MAS NMR) combined with chemometrics to characterize the metabolism of leaves from conventional non-transgenic (NT) and transgenic (T35S) Swingle citrumelo plants overexpressing the P5CSF129A gene, responsible for proline overproduction. This approach enabled the identification of metabolic alterations throughout stress progression. Transgenic plants exhibited constitutive proline accumulation, accompanied by coordinated modulation of choline, fatty acids, glucose, and sucrose. These adjustments reflect the involvement of nitrogen, carbon, and lipid pathways, conferring osmotic and redox stabilities and supporting the maintenance of metabolic homeostasis under severe water deficit. The combination of ^{1}H HR-MAS NMR and chemometrics proved to be a robust, non-destructive chemical tool for elucidating metabolic profiles in genetically modified plants, contributing to the understanding of molecular mechanisms underlying drought tolerance in citrus and supporting the development of rootstocks better adapted to climate change. These findings support the use of ^{1}H HR-MAS NMR metabolomics for elucidating drought-response mechanisms and for advancing omics-driven breeding strategies in citrus.

Keywords: *Citrus*, P5CSF129A gene, 35S promoter, water deficit, proline, ^{1}H HR-MAS NMR

Introduction

Brazil holds a prominent position in global citrus production, being the largest producer of oranges of the world and responsible for more than one-third of the global supply of processed orange juice.[1] According to Citrus Defense Fund (Fundecitrus),[2] the 2023/24 crop from the citrus belt of São Paulo and the Triângulo Mineiro, Southwest Minas Gerais region was estimated at 307.22 million 40.8 kg boxes, corresponding to approximately 12.5 million tons. When other national producing regions are considered, the Brazilian orange crop is forecast to reach approximately 13.5 million metric tons for the 2025/26 marketing year, according to the United States Department of Agriculture Foreign Agricultural Service (USDA/FAS).[3] These figures underscore the economic and strategic relevance of Brazilian citriculture, whose sustainable productivity depends directly on the ability of plants to adapt to regional water and climate variability.[1,4]

However, the citrus industry faces major challenges arising from climate change, particularly with prolonged droughts associated with the El Niño phenomenon, which result in substantial losses in fruit yield and quality.[5] Among the most widely used rootstocks, Rangpur lime (*Citrus limonia* Osbeck), although capable of promoting high productivity, exhibits high susceptibility to diseases such as Citrus Blight and Sudden Death.[6,7] Conversely, Swingle citrumelo (*Citrus paradisi* Macf. × *Poncirus trifoliata* L. Raf.)

*e-mail: glaucia.alcantara@ufms.br
Editor handled this article: Andréa Rodrigues Chaves (Executive)
This publication is part of the special issue "Omics Sciences"

stands out for its resistance to several diseases and its favorable fruit quality, yet it is more sensitive to water deficiency.[7,8] This contrast between biotic resistance and physiological vulnerability has stimulated the search for biotechnological strategies capable of enhancing drought tolerance without compromising other agronomic performances.

Proline is recognized as a multifunctional osmolyte essential to plant responses to abiotic stresses.[9,10] In addition to its role in osmotic adjustment, proline contributes to the stabilization of proteins and membranes and exerts antioxidant functions.[9,11-13] Its biosynthesis from glutamate is catalyzed by the enzyme Δ^1-pyrroline-5-carboxylate synthase (P5CS), whose activity is regulated by feedback inhibition by proline itself.[10,14,15] The P5CSF129A mutation reduces this inhibition, enabling continuous accumulation of the amino acid.[16,17] Thus, introduction of this mutant gene into plants under the control of the constitutive CaMV 35S promoter has proven to be an effective strategy to increase drought tolerance in several species.[10,18,19] In transgenic Swingle citrumelo, P5CSF129A overexpression resulted in increased drought tolerance and enhanced antioxidant activity.[20,21]

Studies[22] conducted by our group demonstrated that transgenic Swingle citrumelo plants exhibit elevated basal levels of proline and proline-betaine accompanied by reduced foliar sucrose, suggesting a redirection of carbon toward the proline biosynthetic pathway. In roots, however, sucrose levels remain stable, contributing to water and energy balance and preventing the excessive accumulation of organic acids.[23-26] Under water stress, these plants maintain higher photosynthetic rates and stomatal conductance compared with non-transgenic plants, indicating that proline acts in an integrated manner to support osmotic homeostasis, redox protection, and metabolic functionality.[12,27-29] The increase in fatty acids observed in plants under drought may reflect both lipid peroxidation and cuticle thickening, mechanisms associated with reduced water loss.[30-32]

Metabolomics has emerged as a powerful tool for the integrated study of plant physiological and biochemical responses, as it directly reflects metabolic alterations driven by genetic and environmental factors.[33-35] Among the available approaches, proton high-resolution magic-angle spinning nuclear magnetic resonance spectroscopy (^{1}H HR-MAS NMR) enables the direct analysis of heterogeneous plant tissues, such as leaves, without the need for prior metabolite extraction, ensuring high reproducibility and preservation of the native chemical state.[36-40]

Despite advances in genetic transformation using P5CSF129A,[18,19] integrated metabolomic studies investigating, in citrumelo, the link between proline overproduction and metabolic behavior during post-stress recovery remain scarce. Therefore, this study aims to evaluate the metabolic profile of conventional and transgenic (T35S) Swingle citrumelo genotypes under different intensities of water stress, using leaf tissues analyzed by ^{1}H HR-MAS NMR combined with chemometric approaches. The underlying premise is that metabolomics, integrated with chemometrics, provides a comprehensive understanding of plant metabolism under abiotic stress conditions, elucidating the chemical interactions among nitrogen-, carbon-, and lipid-based compounds that support drought tolerance.[11,12,31,32]

Experimental

Material

Water stress experiment

The water stress experiment was carried out in a greenhouse under controlled conditions, with an average temperature of 28 ± 2 °C and relative humidity of 69 ± 5%. Swingle citrumelo (*Citrus paradisi* Macf. × *Poncirus trifoliata* L. Raf.) genotypes, conventional non-transgenic (NT) and transgenic (T35S), were used. The transgenic lines were derived from *Agrobacterium tumefaciens*-mediated transformation done by Molinari *et al.*[18] containing the P5CSF129A gene[16] under control of the CaMV 35S promoter,[19] further evaluated by Campos *et al.*[20] and Barichello *et al.*[29] Plants approximately one year old and of uniform size were cultivated in 25 L pots filled with a commercial peat-based organic substrate (Plantmax®), arranged randomly on the bench, and maintained under natural light and controlled irrigation. The experiment followed a completely randomized design with three replicates per genotype, and the total experimental period was 60 days.

Water stress was divided into four physiological stages: without stress (WS), moderate stress (MS), severe stress (SS), and recovery (RE). Stage definition was based on the leaf relative water content (RWC), determined following the method of Weatherley[41] (Table 1) using the equation 1:

$$\mathrm{RWC} = \frac{\text{fresh weight} - \text{dry weight}}{\text{turgid fresh weight}} \times 100 \quad (1)$$

Leaf discs (10 mm of diameter) were weighed immediately after collection (fresh mass), after saturation in distilled water for 24 h (turgid mass), and after oven drying at 60 °C to constant weight (dry mass). After the initial WS sampling, irrigation was suspended until the severe stress stage, then restored for 24 h before sampling during the recovery phase. Leaves from each plant were

collected at the same time of day, immediately frozen in liquid nitrogen, and stored at −80 °C until NMR analysis.

Data collection and analysis

^{1}H HR-MAS NMR analysis

^{1}H HR-MAS NMR analyses were performed on a Bruker Avance III 500 MHz (11.75 T) spectrometer equipped with an HR-MAS probe 4 mm (^{1}H / ^{13}C / ^{31}P / ^{2}H) and pneumatic spinning control at 5 kHz. The care on sample packing and rotor handling were according to Flores *et al*.[42] Leaf samples (9 mg) were cut into small fragments, placed into 50 µL zirconia rotors, and moistened with 30 µL of a 2,2,3,3-d_4 sodium 3-(trimethylsilyl)-propionate and deuterium oxide solution (TMSP-d_4/D_2O, 0.1% m/v).

^{1}H HR-MAS NMR spectra were acquired using the CPMGpr (Carr-Purcell-Meiboom-Gill) pulse sequence at 28 °C with the following parameters: 128 cycles, echo time of 600 µs, relaxation delay (d1) of 2 s, acquisition time (AQ) of 2.18 s, 256 scans (ns), 64k points (TD), and a spectral width (SW) of 30 ppm. The TMSP-d_4 signal at 0.00 ppm was used as the internal reference. For metabolite annotation, two-dimensional HSQC (^{1}H-^{13}C, heteronuclear single quantum coherence) and TOCSY (^{1}H-^{1}H, total correlation spectroscopy) experiments were performed. Chemical shift assignments were based on 2D NMR data, comparison with literature,[22,43-51] and confirmation using the HMDB 3.0 database (2013).[52]

Two-dimensional HSQC experiments were performed using a phase-sensitive pulse sequence, with a spectral width of 5980.86 Hz (12 ppm) in F2 (SWHF2) and 20,831.98 Hz (165.64 ppm) in F1 (SWHF1). The acquisition time (AQ) was 0.09 s, the relaxation delay (d1) was 0.1 s, and the data were acquired with 1k points in F2 (TDF2) and 128 increments in F1 (TDF1). During processing, 1k points (SI) were used in both F2 and F1. Two-dimensional TOCSY experiments were performed using the MLEV composite pulse decoupling sequence, with a spectral width of 5980.86 Hz in both F2 (SWHF2) and F1 (SWHF1). The AQ was 0.34 s, the relaxation delay (d1) was 2.0 s, mixing time of 80 ms, and the data were acquired with 4k points in F2 (TDF2) and 256 increments in F1 (TDF1). During processing, 1k points (SI) were used in both F2 and F1.

Statistical analysis

Spectral data were processed using AMIX 3.9 (Bruker). The 0.4-8.2 ppm region was segmented into 259 buckets of 0.03 ppm, excluding 4.74-4.80 ppm (residual water) and 2.20-2.27 ppm (acetone residue). Integrals were obtained using the special integration mode and normalized to the total spectral area to minimize variations associated with sample mass and instrumental conditions. Principal component analysis (PCA) was applied to explore multivariate patterns and identify discriminant metabolites among experimental groups, using pareto scaling and a 95% confidence level.

Variables highlighted in the loading plots had their relative proportions determined by comparing the area of a representative metabolite signal with that of the TMSP-d_4 standard. Relative areas were subsequently subjected to univariate statistical analysis (one-way ANOVA), followed by test of Tukey (mean comparison) and test of Levene (homogeneity of variance), considering statistical significance at $p < 0.05$.

Results and Discussion

Relative water content in the water stress experiment

According to Table 1, the RWC values obtained for the stress levels were 95% (WS), 82% (MS), 22% (SS), and 88% (RE). The duration of each stress stage (in days), monitored through RWC measurements, is also shown in Table 1. The transgenic genotype (T35S samples) required 37 days to reach moderate stress, whereas the conventional genotype (NT samples) reached this stage in 21 days, indicating greater initial resistance in the transgenic plants. This 76% increase in the duration of the moderate stress stage demonstrates that the metabolism of T35S plants is better able to withstand prolonged periods of water deficit before hydraulic collapse.

Table 1. Relative water content (RWC) in leaves of Swingle citrumelo evaluated at four stages of the water stress experiment and the time required for NT and T35S genotypes to reach the different stress levels based on RWC parameters. Time was measured from the non-stressed stage (start of the experiment, RWC 95%) to moderate stress (RWC 82%), and from moderate to severe stress (RWC 22%). The recovery stage corresponded to 24 h after rewatering

Stress period	RWC / %	Days in each period for NT samples	Days in each period for T35S samples
Without stress (WS)	95	–	–
Moderate stress (MS)	82	21	37
Severe stress (SS)	22	24	21
Recovery (RE)	88	–	–

RWC: relative water content; NT: conventional non-transgenic; WS: without stress; MS: moderate stress; SS: severe stress; RE: recovery.

Spectral profile and visual metabolic variations

The spectral profiles of NT and T35S samples across the different stages of water stress are shown in Figures 1 and 2, respectively. The [1]H HR-MAS NMR spectra displayed signals in characteristic regions corresponding to amino acids and organic acids (0.7-3.0 ppm), osmolytes and nitrogen-containing compounds (3.0-4.0 ppm), carbohydrates (3.0-6.0 ppm), and aromatic compounds (6.0-8.2 ppm). Metabolite assignments are summarized in Table 2 and were confirmed by two-dimensional experiments (HSQC and TOCSY), as shown in the Figures S5 and S6 in the Supplementary Information (SI) section.[22,48,50]

Variations in the intensities of several signals resulting from water stress were observed through visual inspection of the [1]H HR-MAS NMR spectra (Figures S1 and S2, SI section) for NT and T35S genotypes. In the spectra of conventional non-transgenic (NT) Swingle citrumelo leaves (Figure S1, SI section), proline was the metabolite showing the most pronounced variation, with intensified signals at 1.95-2.40 ppm and 3.32-3.45 ppm (overlapped), especially during the severe stress stage. This increase confirms its role as a key osmolyte, acting in the protection of cellular structures, stabilization of proteins, and scavenging of reactive oxygen species.[10-12] It is important to note that proline should be classified as an imino acid rather than an amino acid, since its amino group is secondary due to the cyclization of the side chain with the α-amino group, forming a five-membered ring; its systematic name is pyrrolidine-2-carboxylic acid.

In the transgenic plants (Figure S2, SI section), proline showed elevated levels from the beginning of the water-stress experiment, with little variation during the moderate stress stage and a subsequent increase under severe stress. This elevated proline content in T35S plants even before the onset of stress results from the constitutive expression of the P5CSF129A gene, which converts glutamate into Δ^1-pyrroline-5-carboxylate.[18,22]

Proline betaine (3.11 and 3.30 ppm) partially mirrored the response of proline in both genotypes, though with smaller amplitude (Figures S1 and S2, SI section), confirming its complementary contribution to osmotic balance.[11] In contrast, trimethylamine (2.94 ppm), present in the early stages, was not detected under severe stress. This result is consistent with the metabolic reprogramming that occurs during progressive water deficit, in which many metabolites are differentially regulated throughout the progression of drought, as plants redirect them toward essential osmoprotective and stress-response pathways rather than maintaining the levels of all metabolites.[53-55]

Under water stress, metabolic reprogramming occurs, in which the levels of free nitrogenous metabolites are adjusted as plants prioritize the synthesis of compounds

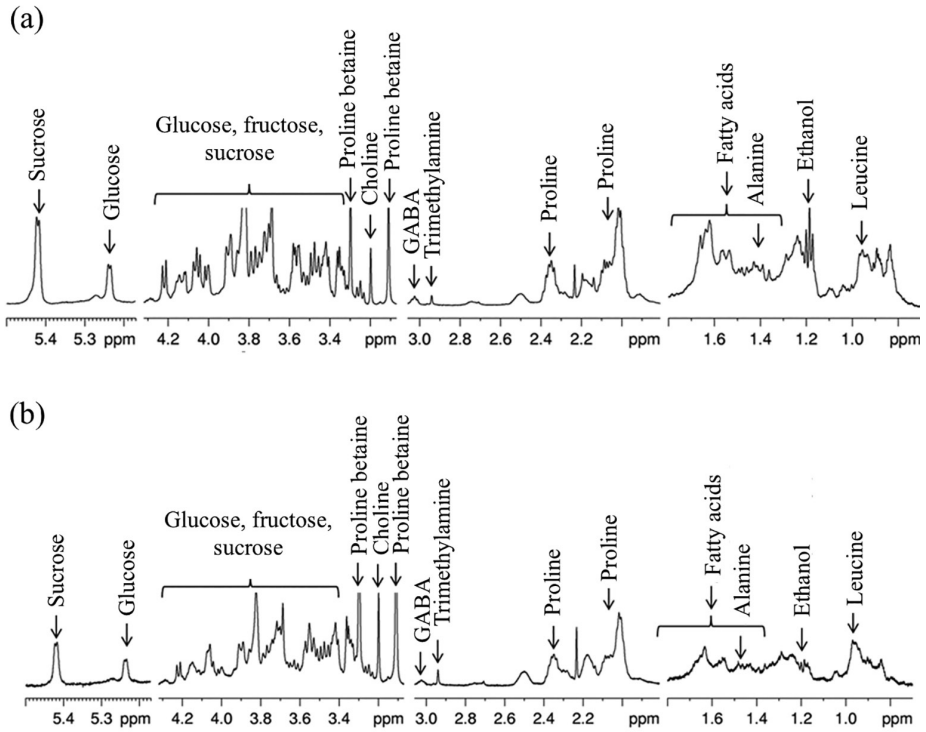

Figure 1. Representative [1]H HR-MAS NMR spectra (500 MHz, suspension in D_2O) of leaves from (a) conventional non-transgenic (NT) and (b) transgenic (T35S) Swingle citrumelo plants.

Table 2. Chemical shift assignments from ^{1}H HR-MAS NMR (500 MHz, suspension in D_2O) for metabolites detected in leaves of both transgenic and conventional non-transgenic Swingle citrumelo plants

Metabolite	^{1}H NMR chemical shift (multiplicity; *J* / Hz) / ppm	^{13}C NMR chemical shift (from ^{1}H-^{13}C HSQC experiment) / ppm	TOCSY (^{1}H-^{1}H correlation)	Stress period			
				WS	MS	SS	RE
Fatty acids	0.81-0.87 (m) 1.27-1.36 (m) 1.59-1.60 (m) 1.97-2.05 (m)	17.0 32.7 [a] [a]	1.27-1.36 1.59-1.60; 1.97-2.05 1.27-1.36 1.27-1.36	D	D	D	D
Alanine	1.49 (d; 6.9) 3.78-3.81 (m)	18.8 [a]	3.78-3.81 1.49	D[c]	D[c]	D[c]	D[a]
Choline	3.20 (s)	57.0		D	D	D	D
Ethanol	1.18 (t; 7.1)	[a]	3.65	D	D	D	D
Fructose	3.54-3.60 (m) 3.70-3.74 (m) 3.88-3.92 (m) 3.96-4.04 (m) 4.10-4.13 (m)	[b] [b] [b] [b] [b]	4.10-4.13 [b] [b] [b] 3.54-3.60	D	D	D	D
GABA	1.89-1.93 (m) 2.27-2.31 (m) 3.02 (t; 7.0)	26.6 28.0 42.5	3.02 [a] 1.89-1.93	D	D	D	D
α-Glucose	4.65 (d; 7.9)	98.9	3.51-3.54; 3.45-3.50; 3.51-3.54	D	D	D	D
β-Glucose	5.24 (d; 3.3) 3.24 (t; 8.2) 3.34-3.38 (m) 3.45-3.50 (m) 3.51-3.54 (m) 3.69-3.80 (m) 3.81-3.92 (m)	95.2 77.2 [b] [b] [b] [b] [b]	3.51-3.54; 3.69-3.80; 3.81-3.92 3.45-3.50 [b] 3.24[b] 5.24[b] 5.24[b] 5.24[b]	D	D	D	D
Leucine	0.93-0.99 (m) 1.66-1.77 (m)	[c] [c]	1.66-1.77 0.93-0.99	D	D	D	D
Proline	1.95-2.12 (m) 2.33-2.40 (m) 3.32-3.38 (m) 3.38-3.45 (m)	26.6 31.2 49.8 49.8	2.33-2.40; 3.32-3.38; 3.38-3.45 1.95-2.12; 3.32-3.38; 3.38-3.45 1.95-2.12; 2.33-2.40 1.95-2.12; 2.33-2.40	D	D	D	D
Proline betaine	3.11(s) 3.30 (s)	49.3 55.5		D	D	D	D
Sucrose	5.42 (d; 3.3) 3.44-3.50 (m) 3.53-3.59 (m) 3.73-3.80 (m) 3.80-3.87 (m) 3.87-3.93 (m) 4.03-4.09 (m) 4.20-4.24 (m)	[a] [b] [b] [b] [b] [b] [b] [b]	[a] [b] [b] [b] [b] [b] [b] [b]	D	D	D	D
Trimethylamine	2.94 (s)	[a]		D	D	ND	D

[a]Not observed; [b]highly overlapped spectral region; [c]metabolite in small proportion;[20] D: detected; ND: not detected; TOCSY: ^{1}H-^{1}H, total correlation spectroscopy; WS: without stress; MS: moderate stress; SS: severe stress; RE: recovery; m: multiplet; s: singlet; t: triplet; d: doublet.

involved in cellular protection and stress responses.[56] In this context, these metabolites may be redirected toward the formation of amino acids associated with osmotic adjustment (e.g., proline and γ-aminobutyric acid (GABA))) or into metabolic pathways that support the production of defense compounds and the maintenance of energy metabolism under conditions of water deficit.[56,57]

Thus, the variation of trimethylamine in this study suggests its association with the transition from the initial metabolic response to stress to a more restricted, survival-oriented state, possibly reflecting adjustments in nitrogen allocation under prolonged water deficit, resulting from metabolic consumption or its redirection to secondary nitrogen compounds.

The anomeric α- and β-signals of glucose and sucrose were detected throughout all stress periods (Figures S1 and S2, SI section), with variations associated with redirected carbon allocation. In T35S, a marked reduction of the sucrose anomeric signal (5.41 ppm) was observed under severe stress, followed by recovery, suggesting the diversion of carbon toward proline biosynthesis, a phenomenon consistent with adaptive metabolic reallocation.[22] Similarly, signals from fatty acids (0.88; 1.27-1.59; 2.02 ppm) increased under severe stress (Figures S1 and S2, SI section). This result indicates intensified synthesis of cuticle and epicuticular waxes as well as controlled lipid peroxidation, mechanisms consistent with protection against water loss.[31,32]

Chemometric analysis of [1]H HR-MAS NMR spectra of conventional non-transgenic (NT) and transgenic (T35S) Swingle citrumelo leaves

Principal component analysis (PCA) was employed to examine the clustering tendency of samples subjected to water stress and to identify the metabolites contributing to each cluster. The PCA biplots revealed clear groupings among the experimental stages, reflecting the metabolic progression of stress and the distinct response capacities of each genotype (Figure 2).

In NT plants, PCA accounted for 88.6% of the total variance, with well-defined separation among the WS, MS, SS, and RE stages. Recovery-phase samples clustered near those from the severe-stress stage, suggesting that metabolic restoration was only partial (Figure 2a).

Based on the combined interpretation of PCA score and loading plots for the NT genotype (Figure 2a), the clustering of WS samples in negative PC1 and positive PC2 was associated with loadings corresponding to choline and proline betaine. Signals attributed to fatty acids and choline grouped the MS samples in positive PC1 and PC2, whereas signals related to proline and lipids (fatty acids) were primarily responsible for clustering the SS samples. In the RE stage, signals assigned to sugars such as glucose, fructose, and sucrose, along with ethanol, contributed to the separation of these samples in negative PC1 and PC2, indicating the resumption of photosynthetic and energetic activity.[58,59]

Among the metabolites highlighted as loadings in the PCA of NT samples (Figure 2a), choline stands out in non-stressed plants due to its essential role in phospholipid membrane synthesis, its contribution to plant development, and its function as a signaling molecule under stress conditions.[60,61] Proline betaine, in turn, acts as an osmolyte that helps maintain cellular water balance and protects proteins and enzymes from damage caused by water and heat stress.[62] However, despite being an osmolyte, proline betaine does not exert the same level of osmoprotective action as proline,[23] which explains why it does not stand out in stressed plants.

Under water stress, oxidative stress also occurs as a consequence of the accumulation of reactive oxygen species (ROS), which promote lipid peroxidation and, consequently, the release of fatty acids derived from the degradation of cellular membranes.[12,63] Additionally, during water deficit, plants may increase the synthesis of lipid compounds and cuticular waxes, resulting in cuticle thickening, a process that contributes to reducing water loss.[64,65] It is plausible that this metabolic pathway represents one of the main sources of the fatty acids highlighted in NT plants under stress (Figure 2a).

Regarding proline in the NT genotype, it becomes prominent during the severe-stress stage because it constitutes the primary plant response to water deficit, contributing to cellular protection by lowering osmotic potential, maintaining water uptake and cell turgor pressure, and thereby sustaining physiological processes.[10,66,67]

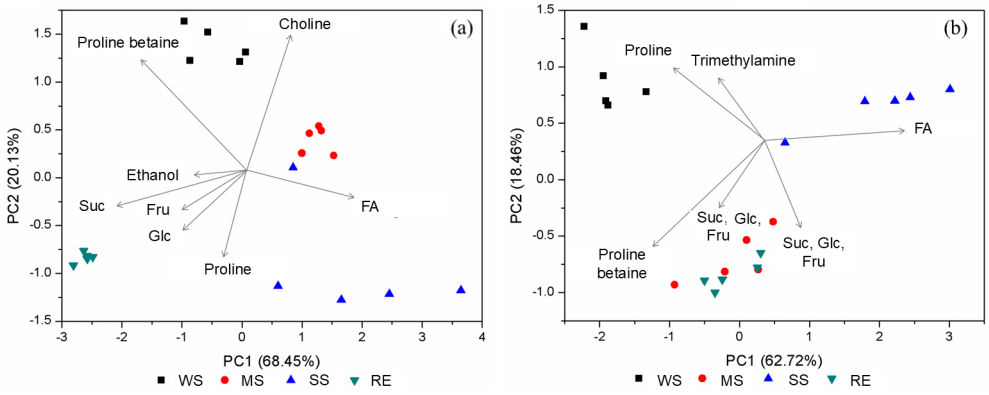

Figure 2. PCA biplot of scores and loadings derived from [1]H HR-MAS NMR spectra of (a) conventional non-transgenic (NT) and (b) transgenic (T35S) Swingle citrumelo leaves under water stress. WS: without stress; MS: moderate stress; SS: severe stress; RE: recovery.

Water stress also reduces photosynthetic activity,[68] ultimately leading to a decline in sugar production. In contrast, plants commonly accumulate sucrose through the hydrolysis of octulose and stachyose, which contributes to the stabilization of molecular interactions during dehydration.[58,69] Accordingly, sugars were prominent during the recovery stage in NT genotype, appearing in higher concentrations and suggesting the reestablishment of photosynthetic activity and carbohydrate biosynthesis.

The presence of ethanol in NT samples during recovery may result from reduced O_2 availability under water deficit, which drives pyruvate metabolism toward fermentative pathways.[70]

For the transgenic T35S plants (Figure 2b), proline was the metabolite most strongly associated with the WS cluster due to its constitutive accumulation. The MS and RE samples were grouped by the loadings of sugars and proline betaine, whereas fatty acids were responsible for the clustering of SS samples, indicating the reinforcement of structural resistance mechanisms under severe stress. This pattern reflects an anticipatory and sustained response in T35S, in contrast to the more reactive and abrupt adjustments observed in NT plants. Proline overproduction likely helped maintain osmotic pressure, delayed stomatal closure, and reduced oxidative stress-effects consistent with the physiological behavior previously reported for transgenic Swingle under drought.[20]

Proline betaine and sugars, along with other minor osmolytes, contribute to stress tolerance by stabilizing cellular structures through hydrophobic interactions and hydrogen bonding.[9,12] As observed in Figure 2b, these metabolites were key loadings during moderate stress in the T35S genotype.

Considering the time required for plants to reach the MS stage (Table 1), it is evident that the osmotic adjustment promoted by proline played a major role in sustaining metabolic processes in T35S. Beyond osmotic regulation, proline mediates tolerance to oxidative stress by scavenging free radicals and ROS, thereby preventing cellular and metabolic damage.[10,12,27]

However, once plants reach a high level of stress, the efficiency of tolerance mechanisms declines. As observed for the conventional genotype, the increased presence of fatty acids is consistent with enhanced cuticle production - which reduces water loss - and with intensified lipid peroxidation triggered by oxidative stress.[30,71]

Finally, the clustering of recovery-stage samples with those under moderate stress (Figure 2b) indicates that, although not yet fully restored, the transgenic plants were gradually returning to their initial metabolic state and recovering more rapidly than the conventional plants (Figure 2a). This enhanced recovery aligns with the elevated proline levels observed in T35S, which help sustain physiological and metabolic processes for longer periods under stress, minimize cellular damage, and support a faster return to pre-stress metabolic conditions.

Relative proportion of metabolites

The analysis of the relative proportions of the metabolites highlighted by PCA strengthened the overall interpretation of the results (Figure 3). Proline was the main differential marker, increasing late in NT plants and constitutively in T35S. Proline betaine partially followed the behavior of proline, whereas choline exhibited pronounced peaks under SS in both genotypes, indicating intensified synthesis of membrane phospholipids (phosphatidylcholine). This is a hallmark of plants exposed to abiotic stress and the remodeling of membranes damaged by lipid peroxidation.[12,72]

Fatty acids showed the largest relative increases under severe stress ($P = 1.74564 \times 10^{-11}$), supporting the hypothesis of cuticular thickening and cell wall reorganization as adaptive responses.[30,31,65] Glucose and sucrose displayed complementary patterns: in NT plants, sucrose accumulation coincided with the late increase in proline, whereas in T35S an earlier rise was observed under MS, which may be associated with macromolecule stabilization and the maintenance of photosynthetic activity (Figure 3).[58]

This synergy among proline, sugars, and lipids reflects the coordinated activation of osmoprotective, antioxidant, and membrane-repair mechanisms, forming the biochemical basis of drought tolerance in the T35S transgenic plants.

In summary, the spectral data (Figures 1, S1 and S2 in the SI section), chemometric analyses (Figures 2, S3 and S4 in the SI section), and relative proportion results (Figure 3; Table 2) demonstrated that the constitutive overproduction of proline in T35S citrumelo promotes a global reconfiguration of metabolism, with shifts in metabolites associated with enhanced osmotic adjustment, oxidative stress protection, and structural reorganization under water deficit.[11,12,20,22] In T35S plants, the maintenance of balanced levels of choline and sugars, combined with moderate and functional accumulation of fatty acids, reflects a regulated and efficient metabolic state, contrasting with the more reactive and less coordinated behavior observed in the conventional NT plants.

Taken together, the evidence confirms that expression of the P5CSF129A gene results in a metabolically resilient plant capable of delaying water loss, minimizing oxidative

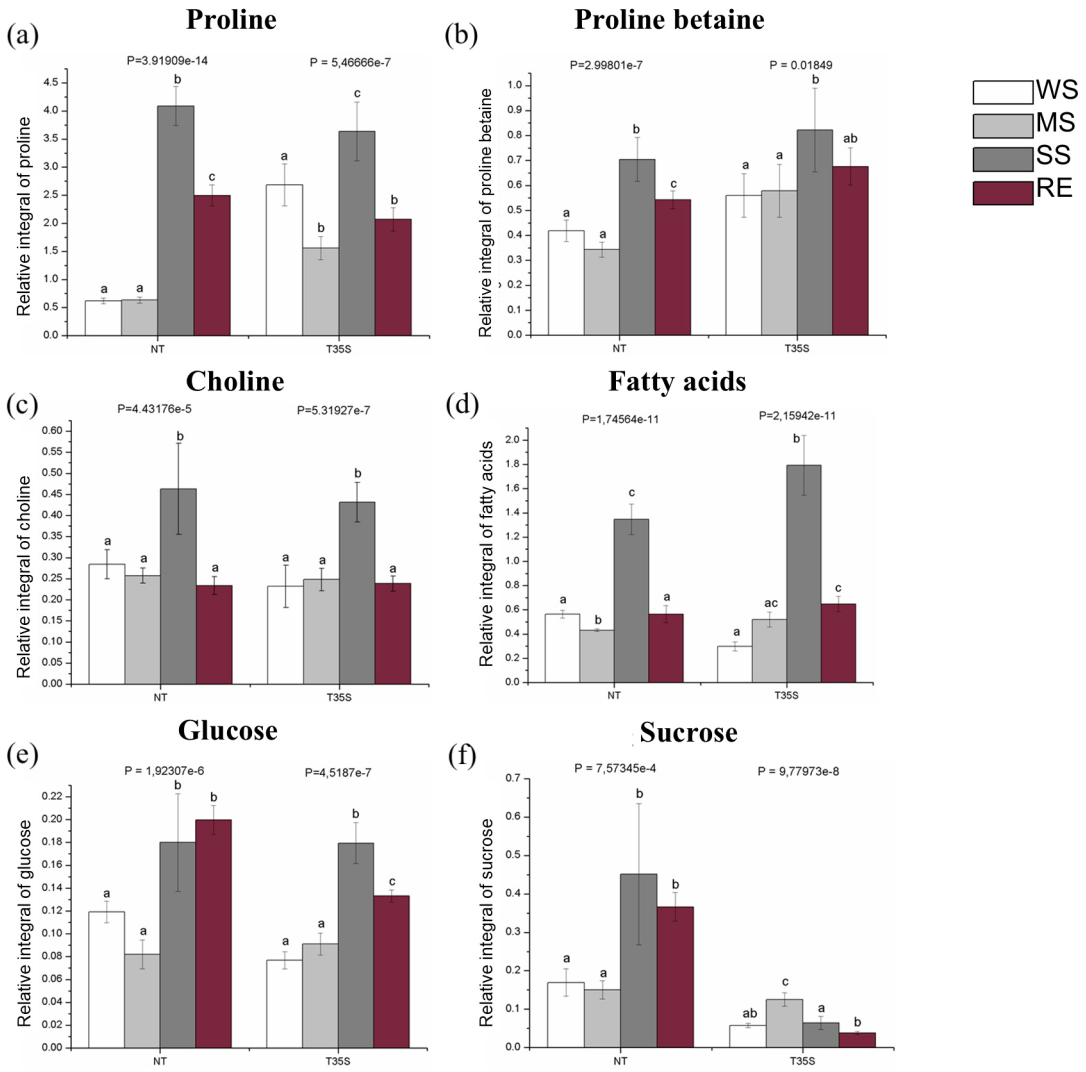

Figure 3. Relative proportion of proline, proline betaine, choline, fatty acids, glucose, and sucrose present in leaves of conventional non-transgenic (NT) and transgenic (T35S) Swingle citrumelo subjected to water stress. Values were determined by integrating the [1]H HR-MAS NMR signals relative to the TMSP reference signal (0.00 ppm). Error bars: ± standard deviation; different letters above the bars indicate significant differences ($P < 0.05$).

stress, preserving photosynthesis, and recovering rapidly upon rehydration.[12,30,31,58,69] Thus, the transgenic Swingle citrumelo T35S emerges as a promising rootstock for citrus production systems in regions subject to water variability and climate change.[20,22,72-74]

Conclusions

The application of [1]H HR-MAS NMR spectroscopy combined with chemometrics enabled the high-resolution characterization of metabolic alterations in leaves of conventional non-transgenic (NT) and transgenic (T35S) Swingle citrumelo throughout the progression of water stress. The direct analysis of *in natura* plant tissues preserved the chemical integrity of metabolites and avoided extraction-related biases, allowing the detection of subtle modifications in osmoprotectants, sugars, and lipids, with clear structural and functional distinctions between genotypes.

The results demonstrated that the constitutive expression of the P5CSF129A gene promotes an integrated reorganization of carbon, nitrogen, and lipid pathways, resulting in the stable accumulation of proline, the main osmoprotective and antioxidant marker. Additionally, the carbon redirection reduces the accumulation of sucrose and glucose under severe water deficit, while the increases in choline and fatty acids indicate membrane-related structural adjustments and cuticular thickening - chemical mechanisms associated with the preservation of cellular integrity. These findings support the use of [1]H HR-MAS NMR metabolomics for elucidating drought-response mechanisms and for advancing omics-driven breeding strategies in citrus

Supplementary Information

Supplementary information is available free of charge at http://jbcs.sbq.org.br as PDF file.

Data Availability Statement

The data that support the findings of this study are available from the corresponding author upon reasonable request.

Acknowledgments

The authors thank financial support provided by the Federal University of Mato Grosso do Sul (UFMS); Fundect/MS (Grant No. 23104.016018/2022-84; 71/020.168/2021; 71/038.233/2022; 71/032.446/2022; 83/026.537/2023), CNPq (Grant No 304860/2024-7; 312595/2021-2; 427221/2018-8); CAPES (Finance Code 001) and FINEP (Grant No. 0113.0358.00).

Author Contributions

C. S. O. was responsible for methodology, data curation, validation, formal analysis, and investigation; P. D. O for data curation and writing (original draft, review and editing); R. P. A fot data curation and writing (original draft); L. G. E. V. and E. F. C. for conceptualization, validation, resources, and writing (review and editing); L. M. L. for conceptualization, methodology, validation, resources, and writing (review and editing); G. B. A. for conceptualization, methodology, data curation, validation, formal analysis, investigation, writing (original draft, review and editing), resources, supervision, and project administration.

References

1. Torsoni, G. B.; Aparecido, L. E. O.; Baratti, A. C.; Rossi, M. F. M.; Lorençone, P. A.; Lorençone, J. A.; *J. Plant Pathol.* **2022**, *33*, 1745. [Crossref]
2. Fundo de Defesa da Citricultura (FUNDECITRUS); *Safra de laranja 2023/24 totalizou 307,22 milhões de caixas de 40,8 kg*. [Link] accessed in October 2025
3. United States Department of Agriculture, Foreign Agricultural Service (USDA/FAS); *Brazil: Citrus Annual – Marketing Year 2025/26*. [Link] accessed in October 2025
4. Rasera, J. B.; da Silva, R. F.; Mourão Filho, F. A. A.; Delbem, A. C. B.; Saraiva, A. M.; Sentelhas, P. C.; Marques, P. A. A.; *Agronomy* **2023**, *13*, 723. [Crossref]
5. Instituto Nacional de Meteorologia (INMET); *El Niño: atuação no Brasil.* [Link] accessed in October 2025
6. Domingues, A. R.; Marcolini, C. D. M.; Gonçalves, C. H. S.; Resende, J. T. V.; Roberto, S. R.; Carlos, E. F.; *Horticulturae* **2021**, *7*, 141. [Crossref]
7. Napoleão, G. M.; Leonel, S.; Souza, J. M. A.; Leonel, M.; Martins, R. C.; Cardoso, C. P.; Tecchio, M. A.; Duarte Filho, J.; *Agriculture* **2023**, *13*, 1551. [Crossref]
8. Silveira, N. M.; de Oliveira, M. I. M.; da Silva, S. F.; Miranda, M. T.; Passos, M. P.; Machado, E. C.; Ribeiro, R. V.; *Braz. J. Bot.* **2024**, *47*, 13. [Crossref]
9. Ghosh, U. K.; Islam, M. N.; Siddiqui, M. N.; Khan, M. A. R.; *Plant Signal Behav*. **2021,** *16*, 1913306. [Crossref]
10. Renzetti, M.; Bertolini, E.; Trovato, M.; *Plants* **2024**, *13*, 1913. [Crossref]
11. Szabados, L.; Savouré, A.; *Trends Plant Sci*. **2010**, *15*, 89. [Crossref]
12. Hossain, M. A.; Hoque, A. M.; Burritt, D. J.; Fujita, M. In *Oxidative Damage to Plants*; Ahmad, P., ed.; Academic Press: London, UK, 2014, p. 477. [Link] accessed in November 2025
13. Raza, A.; Charagh, S.; Abbas, S.; Hassan, M. U.; Saeed, F.; Haider, S.; Sharif, R.; Anand, A.; Corpas, F. J.; Jin, W.; Varshney, R. K.; *Plant Biol. J*. **2023**, *25*, 379. [Crossref]
14. Delauney, A. J.; Verma, D. P. S.; *Plant J.* **1993**, *4*, 215. [Crossref]
15. Verbruggen, N.; Hermans, C.; *Amino Acids* **2008**, *35*, 753. [Crossref]
16. Zhang, C. S.; Lu, Q.; Verma, D. P. S.; *J. Biol. Chem*. **1995**, *270*, 20491. [Crossref]
17. Mushtaq, N. U.; Saleem, S.; Rasool, A.; Shah, W. H.; Tahir, I.; Seth, C. S.; Rehman, R. U.; *Int. J. Genomics* **2025**, 9348557. [Crossref]
18. Molinari, H. B. C.; Bespalhok, J. C.; Kobayashi, A. K.; Pereira, L. F. P.; Vieira, L. G. E.; *Sci. Hortic*. **2004**, *99*, 379. [Crossref]
19. Torres, A. C.; Dusi, A. N.; Santos, M. M.; *Transformação Genética de Plantas via Agrobacterium: Teoria e Prática*; Embrapa Hortaliças: Brasília, Brasil, 2007.
20. Campos, M. K. F.; Carvalho, K.; Souza, F. S.; Marur, C. J.; Pereira, L. F. P.; Bespalhok Filho, J. C.; Vieira, L. G. E.; *Environ. Exp. Bot.* **2011**, *72*, 242. [Crossref]
21. Dubrovna, O. V.; Mykhalska, S. I.; Komisarenko, A. G.; *Cytol. Genet*. **2022**, *56*, 361. [Crossref]
22. Oliveira, C. S.; Carlos, E. F.; Vieira, L. G.; Lião, L. M.; Alcantara, G. B.; *Magn. Reson. Chem*. **2014**, *52*, 422. [Crossref]
23. Nolte, K. N.; Hanson, A. D.; Gage, D. A.; *J. Am. Soc. Hortic. Sci*. **1997**, *122*, 8. [Crossref]
24. Melgar, J. C.; Dunlop, J. M.; Syvertsen, J. P.; *J. Agric. Sci*. **2010**, *148*, 593. [Crossref]
25. Zhang, Y.; Barthe, G.; Grosser, J. W.; Wang, N.; *BMC Genomics* **2016**, *17*, 485. [Crossref]
26. Avico, E. H.; Acevedo, R. M.; Duarte, M. J.; Salvador, A. R.; Nunes-Nesi, A.; Ruiz, O. A.; Sansberro, P. A.; *Plants* **2023**, *12*, 2404. [Crossref]
27. Grant, O. M. In *Abiotic Stress Responses in Plants*; Ahmad, P.; Prasad, M. N. V., eds.; Springer: New York, USA, 2012, ch. 5.

28. Farinacio, R.; Barichello, D.; Andrade, G. A.; Leite, D. A. C.; Santos, C. C. N.; Felicio, M. S.; Campos, M. K. F.; Alcantara, G. B.; Vieira, L. G. E.; Carlos, E. F.; *Citrus R&T.* **2017**, *38*, 2236. [Crossref]
29. Barichello, D.; Farinacio, R.; dos Santos, C. C. N.; Andrade, G. A.; Nagashima, G. T.; Garbúglio, D. D.; Yada, I. F. U.; Travensolo, R. F.; Bianchi, B. C.; Vieira, L. G. E.; Carlos, E. F.; *Citrus Res. Tech.* **2017**, *38*, 1. [Crossref]
30. Balfagón, D.; Segarra-Medina, C.; Rambla, J. L.; Gómez-Cadenas, A.; *Plant Stress.* **2025**, *18*, 101039. [Crossref]
31. Taiz, L.; Zeiger, E.; *Fisiologia Vegetal*, 3rd ed.; Artmed: Porto Alegre, Brazil, 2006.
32. Buchanan, B. B.; Gruissem, W.; Jones, R. L., eds.; *Biochemistry and Molecular Biology of Plants*, 2nd ed.; John Wiley & Sons: Chichester, UK, 2015.
33. Henschel, J. M.; Andrade, E.; dos Santos, J. B. L.; da Silva, R. R.; da Mata, D. A.; Sousa, T.; Batista, D. S.; *Agronomia* **2024**, *14*, 1670. [Crossref]
34. Nicholson, J. K.; Holmes, E.; Lindon, J. C. In *The Handbook of Metabonomics and Metabolomics*; Elsevier: Oxford, UK, 2007, ch. 1.
35. Patti, G. J.; Yanes, O.; Siuzdak, G.; *Nat. Rev. Mol. Cell Biol.* **2012**, *13*, 263. [Crossref]
36. Katam, R.; Lin, C.; Grant, K.; Katam, C. S.; Chen, S.; *Int. J. Mol. Sci*. **2022**, *23*, 6985. [Crossref]
37. Claridge, T. D. W.; *High-Resolution NMR Techniques in Organic Chemistry*; 3rd ed.; Elsevier: Amsterdam, Netherlands, 2009.
38. Viant, M. R.; Ludwig, C.; Günther, U. L. In *Metabolomics, Metabonomics and Metabolite Profiling*; Royal Society of Chemistry: Cambridge, UK, 2007.
39. Alcantara, G. B.; Lião, L. M.; San Gil, R. A. S.; Menezes, S. M. C.; *Ressonância Magnética Nuclear de Alta Resolução com Giro no Ângulo Mágico: Uma Abordagem Teórico-Prática*; v. 5, 1st ed.; AUREMN: Rio de Janeiro, Brasil, 2014.
40. Augustijn, D.; de Groot, H. J. M.; Alia, A.; *Molecules* **2021**, *26*, 931. [Crossref]
41. Weatherley, P. E.; *New Phytol.* **1950**, *49*, 81. [Crossref]
42. Flores, I. S.; Martinelli, B. C. B.; Pinto, V. S.; Queiroz Jr., L. H. K.; Lião, L. M.; *Phytochem. Anal*. **2019**, *30*, 5. [Crossref]
43. Gall, L. G.; Colquhoun, I. J.; Davis, A. L.; Collins, G. J.; Verhoeyen, M. E.; *J. Agric. Food Chem.* **2003**, *51*, 2447. [Crossref]
44. Defernez, M.; Gunning, Y. M.; Parr, A. J.; Shepherd, L. V.; Davies, H. V.; Colquhoun, I. J.; *J. Agric. Food Chem.* **2004**, *52*, 6075. [Crossref]
45. Sobolev, A. P.; Brosio, E.; Gianferri, R.; Segre, A. L.; *Magn. Reson. Chem.* **2005**, *43*, 625. [Crossref]
46. Choi, H-K.; Yoon, J.-H.; Kim, Y.-S.; Kwon, D. Y.; *Process Biochem*. **2007**, *42*, 263. [Crossref]
47. Pérez, E. M. S.; Iglesias, M. J.; Ortiz, F. L.; Pérez, I. S.; *Food Chem.* **2010**, *122*, 877. [Crossref]
48. Bharti, S. K.; Bhatia, A.; Tewari, S. K.; Sidhu, O. P.; Roy, R.; *Magn. Reson. Chem*. **2011**, *49*, 659. [Crossref]
49. Georgiev, M. I.; Ali, K.; Alipieva, K.; Verpoorte, R.; Choi, Y. H.; *Phytochemistry* **2011**, *72*, 2045. [Crossref]
50. Silva, L. M. A.; Alves Filho, E. G.; Choze, R.; Lião, L. M.; Alcantara, G. B.; *J. Braz. Chem. Soc*. **2012**, *23*, 1054. [Crossref]
51. Lee, S. Y.; Lee, S.; Lee, S.; Oh, J. Y.; Jeon, E. J.; Ryu, H. S.; Lee, C. H.; *Food Chem*. **2014**, *15*, 165. [Crossref]
52. Wishart, D. S.; Jewison, T.; Guo, A. C.; Wilson, M.; Knox, C.; Liu, Y.; Djoumbou, Y.; Mandal, R.; Aziat, F.; Dong, E.; Bouatra, S.; Sinelnikov, I.; Arndt, D.; Xia, J.; Liu, P.; Yallou, F.; Bjorndahl, T.; Perez-Pineiro, R.; Eisner, R.; Allen, F.; Neveu, V.; Greiner, R.; Scalbert, A.; *Nucleic Acids Res*. **2013**, *41*, D801. [Crossref]
53. Skirycz, A.; Inzé, D.; *Curr. Opin. Biotechnol*. **2010**, *21*, 197. [Crossref]
54. Bowne, J. B.; Erwin, T. A.; Juttner, J.; Schnurbusch, J.; Langridge, P.; Bacic, A.; Roessner, U.; *Mol. Plant* **2012**, *5*, 418. [Crossref]
55. Falcioni, R.; Oliveira, C. A.; Vedana, N. G.; Mendonça, W. A.; Gonçalves, J. V. F.; Haubert, D. F. S.; de Matos, D. H. S.; Reis, A. S.; Antunes, W. C.; Crusiol, L. G. T.; Sibaldelli, R. N. R.; Nepomuceno, A. L.; Neumaier, N.; Farias, J. R. B.; Furlanetto, R. H.; Demattê, J. A. M.; Nanni, M. R.; *Plants* **2025**, *14*, 2615. [Crossref]
56. Zeljković, S. C.; De Diego, N.; Drašar, L.; Nisler, J.; Havlíček, L.; Spíchal, L.; Tarkowski, P.; *J. Exp. Bot*. **2024**, *75*, 5390. [Crossref]
57. Hildebrandt, T. M.; Nunes, N. A.; Araújo, W. L.; Braun, H. P.; *Mol. Plant* **2015**, *8*, 1563. [Crossref]
58. Farrant, J. M.; Brandt, W.; Lindsey, G. G.; *Plant Stress* **2007**, *1*, 72. [Crossref]
59. Yu, J.; Zhang, R.; Li, X.; Dong, D.; Wang, S.; *Agronomy* **2025**, *15*, 320. [Crossref]
60. Paper, J. M.; Mukherjee, T.; Schrick, K.; *Plant Methods* **2018**, *14*, 1. [Crossref]
61. Zhang, K.; Lyu, W.; Gao, Y.; Zhang, X.; Sun, Y.; Huang, B.; *Plant Cell Physiol.* **2020**, *61*, 2018. [Crossref]
62. Ashraf, M.; Foolad, M. R.; *Environ. Exp. Bot*. **2007**, *59*, 206. [Crossref]
63. Mittler. R.; *Trends Plant Sci*. **2017**, *22*, 11. [Crossref]
64. Wang, X.; Kong, L.; Zhi, P.; Chang, C.; *Int. J. Mol. Sci*. **2020**, *21*, 5514. [Crossref]
65. Fakhrzad, F.; Jowkar, A.; *BMC Plant Biol.* **2024**, *24*, 330. [Crossref]
66. Yancey, P. H.; *J. Exp. Biol.* **2005**, *208*, 2819. [Crossref]
67. Luo, Q.; Ma, Y.; Xie, H.; Chang, F.; Guan, C.; Yang, B.; Ma, Y.; *Plants* **2024**, *13*, 1408. [Crossref]

68. Morade, A. S.; Sharma, R. M.; Dubey, A. K.; Sathee, L.; Kumar, S.; Kadam, D. M.; Awasthi, O. P.; Kumar, A.; Yadav, D.; *BMC Plant Biol*. **2025**, *25*, 753. [Crossref]
69. Khan, M. A.; Liu, D. H.; Alam, S. M.; Zaman, F.; Luo, Y.; Han, H.; Ateeq, M.; Liu, Y. Z.; *Plant Physiol. Biochem*. **2023**, *203*, 108056. [Crossref]
70. Bui, L. T.; Novi, G.; Lombardi, L.; Iannuzzi, C.; Rossi, J.; Santaniello, A.; Mensuali, A.; Corbineau, F.; Giuntoli, B.; Perata, P.; Zaffagnini, M.; Licausi, F.; *J. Exp. Bot*. **2019**, *70*, 1815. [Crossref]
71. Sharma, P.; Lakra, N.; Goyal, A.; Ahlawat, Y. K.; Zaid, A.; Siddique, K. H. M.; *Front. Plant Sci*. **2023**, *10*, 1216835. [Crossref]
72. Guo, Q.; Liu, L.; Barkla, B. J.; *Int. J. Mol. Sci*. **2019**, *20*, 4264. [Crossref]
73. Zuo, Z.-F.; Li, Y.; Mi, X.-F.; Li, Y.-L.; Zhai, C.-Y.; Yang, G.-F.; Wang, Z.-Y.; Zhang, K.; *Front. Plant Sci*. **2023**, *14*, 1269286. [Crossref]
74. Nakabayashi, R.; Saito, K.; *Curr. Opin. Plant Biol*. **2015**, *24*, 10. [Crossref]

Submitted: December 7, 2025
Accepted Article online: March 22, 2026
Final version online: April 14, 2026